RAPID COMMUNICATIONS

PHYSICAL REVIEW D VOLUME 41, NUMBER 7 1 APRIL 1990

Test of scaling of the massive-dihadron cross section

D. M. Kaplan and R. Guo*
Northern Illinois University, DeKalb, Illinois 60115

C. N. Brown and W. E. Cooper
Fermi National Accelerator Laboratory, Batavia, Illinois 60510

M. J. Wang
Case Western Reserve University, Cleveland, Ohio 44106

T. A. Carey, M. J. Leitch, P. L. McGaughey, C. S. Mishra,† J. M. Moss, and J.-C. Peng
Los Alamos National Laboratory, Los Alamos, New Mexico 87545

M. L. Barlett and G. W. Hoffmann
University of Texas, Austin, Texas 78712

(Received 29 December 1989)

Measurements of the cross section for production of massive dihadrons by 800-GeV protons incident on a tungsten target are presented. These are compared with measurements taken at lower and higher $\sqrt{s}$ and with perturbative-QCD predictions. Scaling and A-dependence behaviors observed at lower energies are confirmed, and good agreement with QCD is obtained. Model dependences of earlier measurements are discussed.

In the late 1970s, the Columbia–Fermilab–Stony Brook (CFS) group studied production of pairs of high-transverse-momentum hadrons in collisions of 200-, 300-, and 400-GeV protons with beryllium and tungsten targets,[1–4] and the Columbia-CERN-Oxford-Rockefeller (CCOR) group studied production of π^0 pairs at the CERN ISR.[5] We have taken new dihadron data using 800-GeV protons incident on a tungsten target. We find that the scaling behavior and A dependence observed by CFS are corroborated at the higher energy, but that one of the CFS publications[1] contains a misleading figure.

We utilized the Fermilab E605/772 spectrometer (Fig. 1), the details of which have been published.[6] For this run, we added a collimator at the exit of the "SM12"

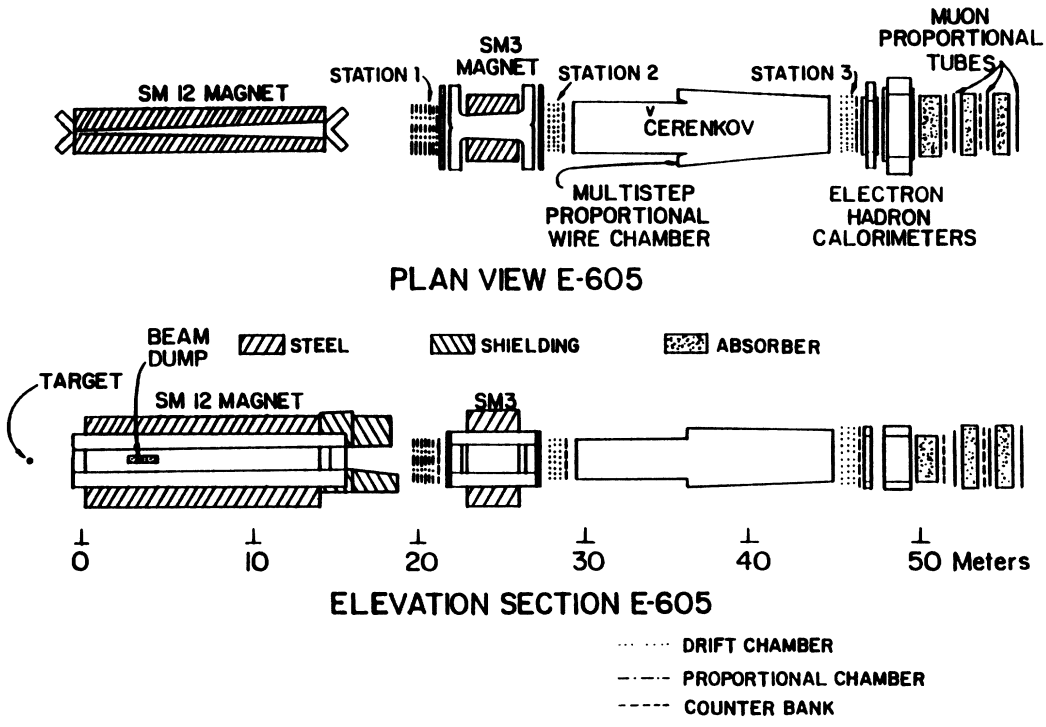

FIG. 1. Schematic diagram of the E605/772 spectrometer.

analyzing magnet, composed of 24 in. of copper followed by 48 in. of borated polyethylene, that restricted the vertical aperture to ±10 in. The tungsten-disk target, of thickness 3 mm and diameter 3 in., was struck by 2.5×10^{10} protons per 20-s beam pulse. Since the diameter of the target was much larger than the size of the beam, the targetting efficiency was 100%.

The beam flux was measured with a secondary emission monitor (SEM) located upstream of the target. For calibration, the SEM rate was compared with the production rate of ^{24}Na in copper foils; the calibration has been stable within ±5% for several years. Integrated proton fluxes are derived using a ^{24}Na production cross section[7] of 3.9 mb per Cu nucleus. Note that CFS used a 10% lower value measured at Brookhaven,[8] since measurements at Fermilab energies were not then available. We use this older value when comparing to CFS.

The data presented here satisfied a "low-bias" trigger which was prescaled by a factor of 8 or 16. The trigger required at least 50 GeV of energy deposition in the hadron calorimeter and coincident hits in three out of four hodoscope planes both on the left and right sides of the vertical centerline of the spectrometer. For 43 922 prescaled low-bias events written to tape, corresponding to 1.2×10^{11} incident protons, 3404 were found to contain two oppositely charged hadron tracks. These tracks were traced back through the magnetic field of SM12, and fiducial cuts were imposed to eliminate tracks passing too close to shielding material. The 2516 remaining pair events were cut on the vertical and horizontal positions at the target, to eliminate events due to upstream vacuum windows or the downstream beam dump. For each of the 437 remaining events, the intersection point of the track pair was computed in the y-z (magnetic bend) view and the x-z (nonbend) view. Figure 2 shows the distribution of these points along the z axis (incident beam direction) in the two views. The target is seen clearly in both views. Figure 3 shows the mass and pair-p_t distributions of these events, and Fig. 4 shows the pair-p_t distribution in two bins of mass 5–6 GeV and 6–7 GeV.

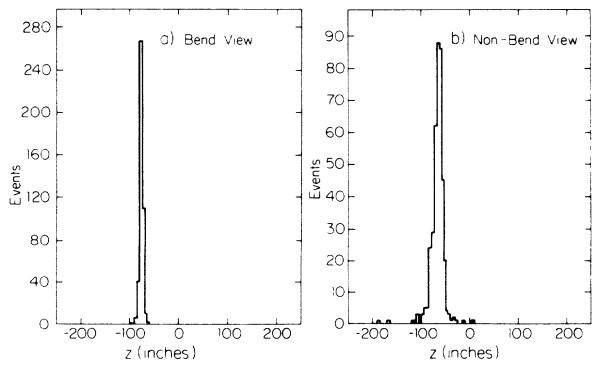

FIG. 2. Reconstructed z_{target} distributions in magnetic bend (y-z) and nonbend (x-z) views. The target was located at $z = -80$ in.

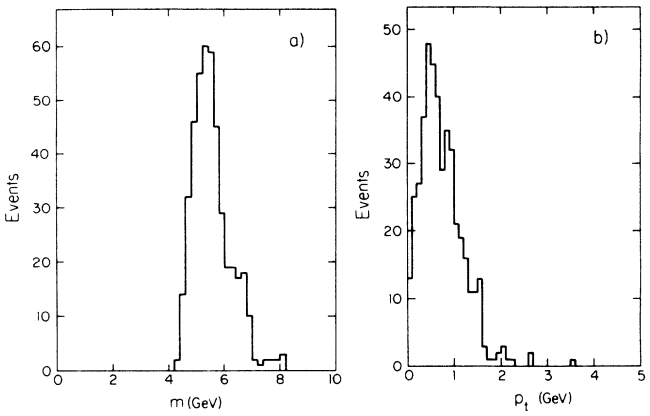

FIG. 3. Distribution of observed events vs mass and pair p_t.

Our efficiencies for recording and reconstructing these events are all high. Electronic dead time caused a 13.7% loss of beam. The trigger allowed any one of four hodoscope elements to be missing on each of the right and left sides, and the hodoscope counter efficiencies were all over 95%, so we make no correction for trigger counter efficiency. The calorimeter energy threshold was well below the geometric turn-on of the magnetic spectrometer acceptance (the lowest observed total momentum of a target-originated hadron pair was 90 GeV), so we make no correction for calorimeter trigger efficiency.[9] The track reconstruction allowed up to seven of the 18 chamber planes to be missing (not more than three at any one of the three measurement stations), and the chamber efficiencies were all over 90%. The most likely number of planes per track was observed to be 17, and the measured reconstruction efficiency was 0.997 per track. We make no correction for tracking efficiency. At an early stage of analysis, events containing more than two tracks were eliminated from the data sample, amounting to 6% of events having two or more tracks. Since many of these

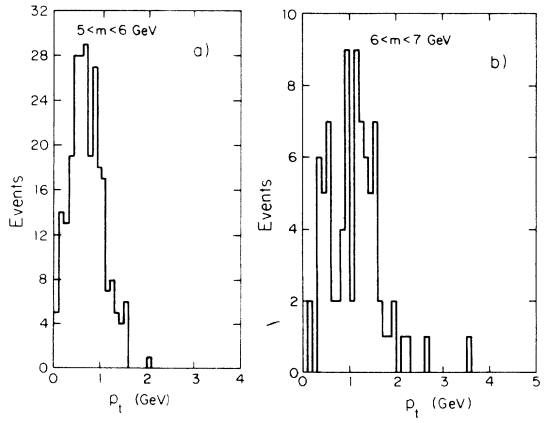

FIG. 4. Event distributions vs pair p_t: (a) $5 < m < 6$ GeV, (b) $6 < m < 7$ GeV.

events were probably not of target origin, we correct our cross sections upwards by 3% and assign a ±3% error contribution on the overall normalization to this source.

The spectrometer acceptance is defined as the fraction of produced events in a given kinematic bin which traverse the open aperture of the spectrometer and pass through all of the detectors. We compute it by Monte Carlo simulation, using a dihadron production model which has been iterated to agree with the observed distributions. To convert these distributions into cross sections nevertheless requires some knowledge of the production distributions in regions not covered by our spectrometer. Figure 5 shows the spectrometer acceptance versus mass, pair p_t, center-of-mass rapidity, and dihadron-rest-frame (Collins-Soper) polar angle (θ^*). Like the CFS spectrometer, the E605/772 spectrometer covers only narrow regions in rapidity and polar angle, and its acceptance falls rapidly with increasing pair p_t. We therefore follow the CFS convention and report cross sections differential in rapidity averaged over our rapidity interval. In comparing with CFS cross sections, we make the conventional assumption, appropriate to the production and decay into dihadrons of a hypothetical resonance, of isotropic distribution in $\cos\theta^*$. As an alternative we also present the cross section differential in $\cos\theta^*$. Since the acceptance versus mass depends on the assumed p_t production distribution (larger for a narrow p_t distribution and smaller for a broad one), we consider first the invariant differential dihadron cross section versus pair p_t, which does not suffer from this model dependence. Figure 6(a) shows

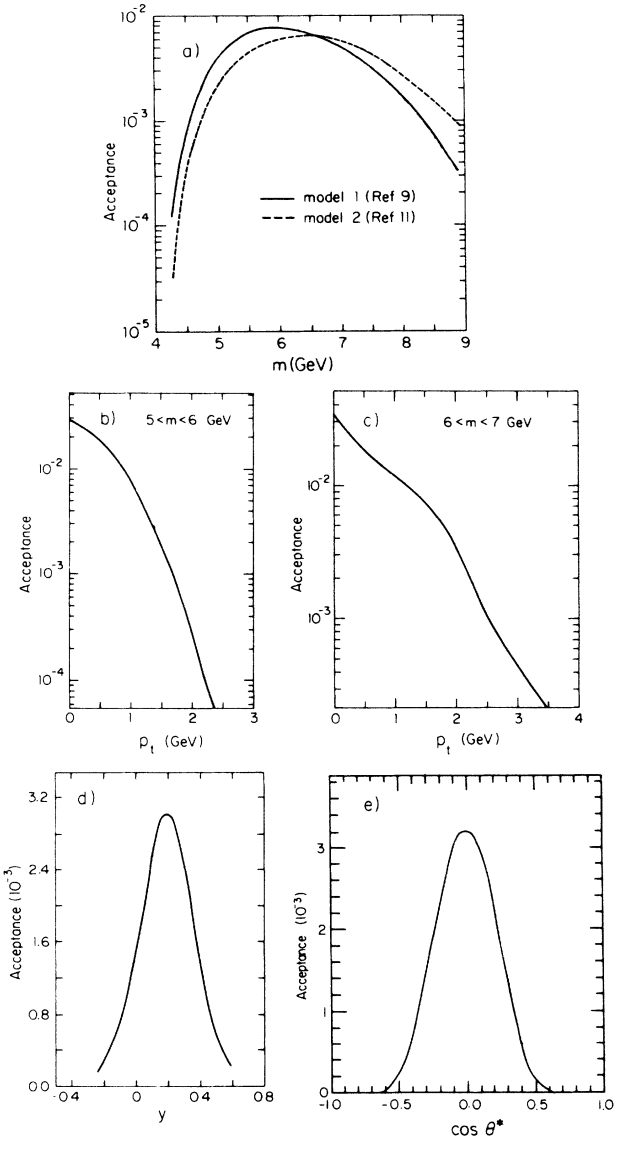

FIG. 5. Spectrometer acceptance vs (a) mass (for two assumed p_t distributions; see text), (b) pair p_t ($5 < m < 6$ GeV), (c) pair p_t ($6 < m < 7$ GeV), (d) center-of-mass rapidity, (e) cosine of Collins-Soper-frame polar angle.

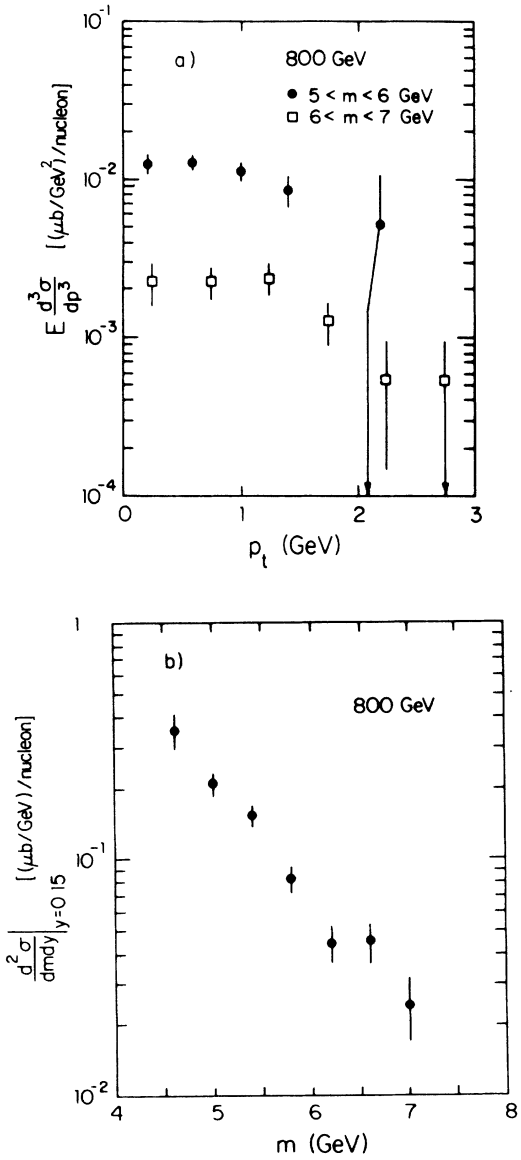

FIG. 6. Differential cross sections vs (a) pair p_t and (b) mass.

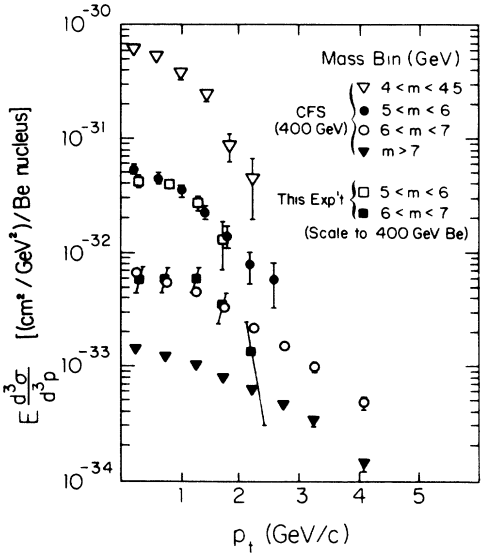

FIG. 7. Comparison of invariant cross section for hadron-pair production vs pair p_t from this experiment, scaled as described in text, with that of CFS (Ref. 1).

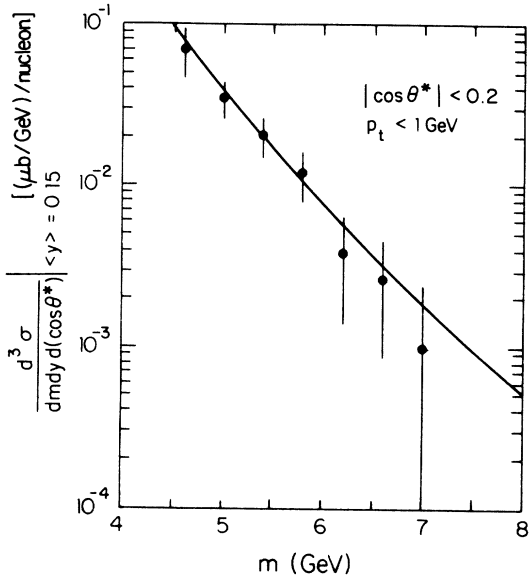

FIG. 9. Triply-differential cross section for hadron-pair production vs mass. The curve is the prediction of the QCD model of J. F. Owens (Ref. 12).

this cross section in two bins of mass.

To compare with 400-GeV CFS cross sections per beryllium nucleus, we scale according to the linear nucleon-number (A) dependence which CFS observed.[2,4] We correct for our higher beam energy according to the CFS fit to the beam-energy dependence[4] $\sigma \propto (1 - m/\sqrt{s})^{13.0\pm0.4}$. Figure 7 compares the resulting cross sections with those of Ref. 1, Fig. 3. The good agreement verifies the p_t dependence observed by CFS as well as the s and A dependences.

We have parametrized[10] the observed[1] CFS p_t dependence to compute the acceptance versus mass (solid curve in Fig. 5). Figure 6(b) gives the resulting cross section $d^2\sigma/dm\,dy$, averaged over our rapidity interval $-0.26 < y < 0.46$. In Fig. 8, we compare this cross section, scaled as above for the s and A dependence, with that of Ref. 1, Fig. 2. The scaled 800-GeV cross section is in substantial disagreement with the CFS 400-GeV cross section (lower by a factor ranging from 10 at low mass

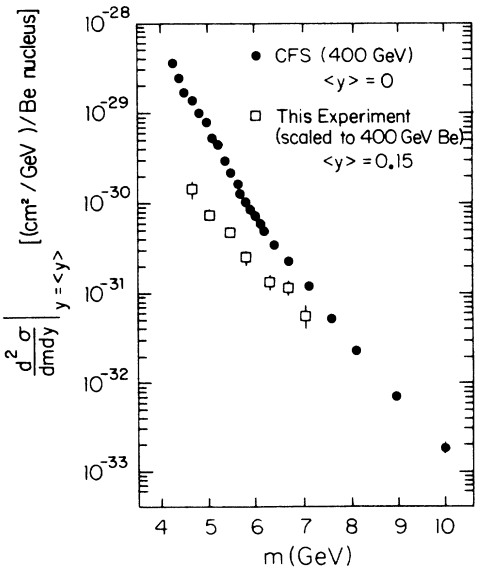

FIG. 8. Comparison of differential cross section for hadron-pair production vs mass from this experiment, scaled as described in text, with that of CFS (Ref. 1).

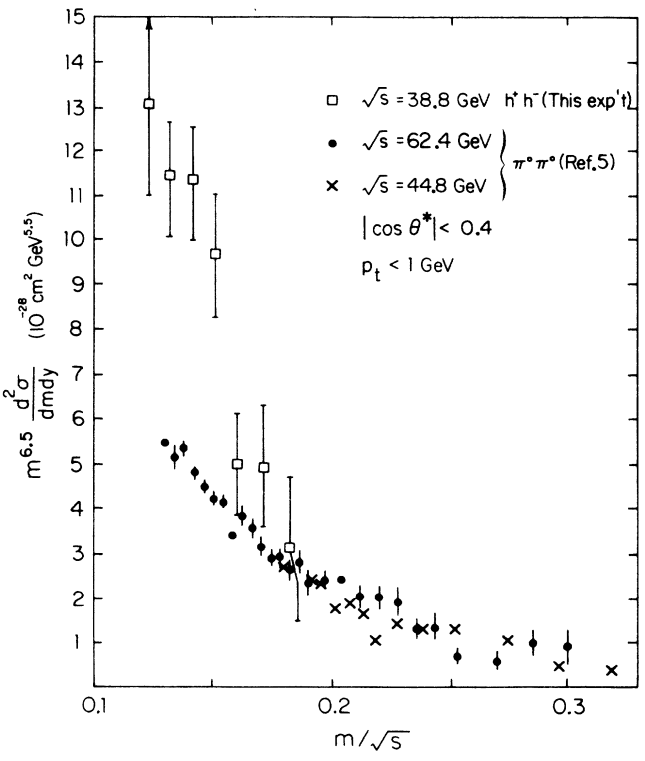

FIG. 10. Comparison of differential cross section for hadron-pair production vs mass from this experiment, scaled as described in text, with that of CCOR (Ref. 5).

to 3 at high mass). To develop some insight into this discrepancy, we have also tried in the Monte Carlo simulation a parametrization similar to that used by CFS[11] in Ref. 1 (which however, is inconsistent with the CFS data), based on measurements at Brookhaven Alternating Gradient Synchrotron energy.[12] The resulting acceptance, indicated by the dashed curve in Fig. 5, is a factor of 2 to 3 lower at low mass but 30% higher at high mass than the acceptance computed above. Since the CFS acceptance varied even more rapidly with p_t than does ours,[4] we conclude that their sensitivity to the assumed p_t model was even greater, and this may explain the disagreement shown in Fig. 8.

We can compute a cross section which is less model dependent by restricting the pair-p_t and θ^* ranges. Figure 9 presents such a cross section, $d^3\sigma/dm\,dy\,d(\cos\theta^*)$, integrated over the range $0 < p_t < 1$ GeV and averaged over $-0.2 < \cos\theta^* < 0.2$. Also shown is the prediction of the QCD model of Owens,[13] which was tuned to agree with the CCOR data, and which is seen to agree with our data as well.

We also compare our results directly to those of CCOR.[5] They measured the production of pairs of π^0's in proton-proton collisions at $\sqrt{s} = 44.8$ and 62.4 GeV. They report a cross section differential in mass and rapidity and integrated over the range $p_t < 1$ GeV, $-0.4 < \cos\theta^* < 0.4$. Their observed $\cos\theta^*$ dependence is parametrized as $dN/d(\cos\theta^*) \propto (1 - \cos\theta^*)^{-a} + (1 + \cos\theta^*)^{-a}$, with $a = 2.97 \pm 0.05$, independent of mass and $\sqrt{s}$. We use this fit to extrapolate our cross section over their $\cos\theta^*$ range. The result is shown in Fig. 10, plotted in the CCOR scaling form $m^{6.5}d^2\sigma/dm\,dy$, along with the CCOR data. Our data lie higher than CCOR's by about a factor of 2, as would be expected from simple quark-counting arguments. We have also compared our data with preliminary results from Fermilab E711[14] covering the range 6 GeV$< m <$15 GeV, and we find excellent agreement in the region of overlap.

The new data confirm that the dihadron cross section near $y = 0$ and $p_t = 0$ shows a simple scaling behavior with energy. The results differential (Fig. 7) or restricted (Fig. 9) in pair p_t should have the smallest systematic normalization uncertainty, which we estimate to be $\pm 20\%$. Cross sections integrated over all p_t have greater uncertainty, due to the poorly known pair-p_t dependence at large p_t. This may help to explain the large discrepancy seen in Fig. 8.

We thank J. Owens, D. Levinthal, and J. Bjorken for useful discussions. This work was supported in part by the U. S. Department of Energy.

---

*Present address: University of Illinois at Chicago, Chicago, IL 60680.

†Present address: Fermilab, Batavia, IL 60510.

[1] R. D. Kephart *et al.*, Phys. Rev. Lett. **39**, 1440 (1977).

[2] R. L. McCarthy *et al.*, Phys. Rev. Lett. **40**, 213 (1978).

[3] R. J. Fisk *et al.*, Phys. Rev. Lett. **40**, 984 (1978).

[4] H. Jöstlein *et al.*, Phys. Rev. D **20**, 53 (1979).

[5] A. L. S. Angelis *et al.*, Nucl. Phys. **B209**, 284 (1982).

[6] Y. B. Hsiung *et al.*, Phys. Rev. Lett. **55**, 457 (1985); J. A. Crittenden *et al.*, Phys. Rev. D **34** 2584, (1986); D. M. Kaplan, in *Quark, Strings, Dark Matter, and All the Rest*, proceedings of the Conference, Nashville, Tennessee, 1986, edited by R. S. Panvini and T. J. Weiler (World Scientific, Singapore, 1987), p. 83.

[7] S. Baker *et al.*, Nucl. Instrum. Methods **222**, 467 (1984).

[8] J. Hudis *et al.*, Phys. Rev. **129**, 434 (1963); J. B. Cumming *et al.*, Phys. Rev. C **14**, 1554 (1976).

[9] D. E. Jaffe *et al.* [Phys. Rev. D **40**, 2777 (1989)] and D. E. Jaffe (Ph.D. thesis, SUNY at Stony Brook, 1987) show that the calorimeter trigger efficiency reached 100% by 120 GeV for the "*EHI*" trigger, for which an 8-dB resistive attenuator was inserted before the trigger discriminator. The present data were obtained with 0-dB attenuation and hence 100% efficiency by 50 GeV.

[10] $dN/dp_t \propto p_t\ e^{-[p_t^2/b(m)]}$, $b(m) = 1.27(0.16m^2 - 1.23m + 3.48)^2$.

[11] R. D. Kephart (private communication).

[12] $dN/dp_t \propto p_t\ e^{-bT}$, where $T \equiv \sqrt{m^2 + 1.5p_t^2} - m$, from J. J. Aubert *et al.*, Phys. Rev. Lett. **35**, 639 (1975). Following CFS, we choose $b = 1.6$.

[13] J. F. Owens (private communication); and in *The Storrs Meeting*, proceedings of the 1988 Meeting of the Division of Particles and Fields of the APS, edited by K. Haller *et al.* (World Scientific, Singapore, 1989), p. 570.

[14] K. Streets, Ph.D. dissertation, Florida State University, 1989.